Transcriptome Analysis of *Drosophila* CNS Midline Cells Reveals Diverse Peptidergic Properties and a Role for *castor* in Neuronal Differentiation

Joseph R. Fontana and **Stephen T. Crews**[*]
Department of Biochemistry and Biophysics, Program in Molecular Biology and Biotechnology, The University of North Carolina at Chapel Hill, Chapel Hill, NC 27599-3280

Abstract

One of the key aspects of neuronal differentiation is the array of neurotransmitters and neurotransmitter receptors that each neuron possesses. One important goal of developmental neuroscience is to understand how these differentiated properties are established during development. In this paper, we use fluorescence activated cell sorting and RNA-seq to determine the transcriptome of the *Drosophila* CNS midline cells, which consist of a small number of well-characterized neurons and glia. These data revealed that midline cells express 9 neuropeptide precursor genes, 13 neuropeptide receptor genes, and 31 small-molecule neurotransmitter receptor genes. In situ hybridization and high-resolution confocal analyses were carried-out to determine the midline cell identity for these neuropeptides and the neuropeptide receptors. The results revealed a surprising level of diversity. Neuropeptide genes are expressed in a variety of midline cell types, including motoneurons, GABAergic interneurons, and midline glia. These data revealed previously unknown functional differences among the highly-related iVUM neurons. There also exist segmental differences in expression for the same neuronal sub-type. Similar experiments on midline-expressed neuropeptide receptor genes reveal considerable diversity in synaptic inputs. Multiple receptor types were expressed in midline interneurons and motoneurons, and, in one case, link feeding behavior to gut peristalsis and locomotion. There were also segmental differences, variations between the 3 iVUMs, and three hormone receptor genes were broadly expressed in most midline cells. The *Drosophila* Castor transcription factor is present at high levels in iVUM5, which is both GABAergic and expresses the *short neuropeptide F precursor* gene. Genetic and misexpression experiments indicated that *castor* specifically controls expression of the *short neuropeptide F precursor* gene, but does not affect iVUM cell fate or expression of *Gad1*. This indicates a novel function for *castor* in regulating neuropeptide gene expression.

Keywords

castor; CNS midline; *Drosophila*; FACS; neuropeptide; RNA-seq

[*]Author for correspondence: steve_crews@unc.edu, Tel: 919-962-4380, Fax: 919-962-8472.

Introduction

One of the key goals of developmental neuroscience is to understand the origins of neuronal and glial diversity. One of the important characteristics of differentiated neurons is their complement of neurotransmitters and neurotransmitter receptors. By coupling the isolation of specific CNS cell types and RNA-seq transcriptomic analysis with in situ hybridization/ immunostaining of expressed genes, it is possible to characterize the differentiated properties of individual CNS cells. In this manner the following questions can be addressed: (1) do individual neurons express multiple neurotransmitters and neurotransmitter receptors, (2) how similar are different types of neurons (e.g. dopaminergic vs. GABAergic neurons), (3) how similar are related neurons (e.g. dopaminergic neurons in distinct regions of the CNS), (4) do homologous neurons differ in different segments or regions, (5) do glia express neurotransmitter or neurotransmitter receptors, and (6) what are the regulatory mechanisms that control differentiation? In this paper, we isolate a small set of neurons and glia that reside at the midline of the *Drosophila* embryonic CNS, perform RNA-seq to define the midline transcriptome, validate the information with high-resolution in situ hybridization to determine the cell-type specificity of each gene, and identify a transcriptional regulator of a peptide neurotransmitter.

The *Drosophila* CNS midline cells have been well-characterized and provide an excellent system to study the genetic origins of neuronal and glial diversity. In the late stage embryonic CNS, there are ~22 midline cells per segment (Fig. 2B). These include 2 peptidergic MP1 neurons, the dopaminergic H-cell interneuron, the glutamatergic H-cell sib interneuron, 3 GABAergic iVUM (Ventral Unpaired Median interneurons) interneurons, and 3 octopaminergic/glutamatergic mVUM motoneurons that innervate body wall muscles and the female reproductive system (Wheeler et al., 2006). These neurons are derived from a set of Midline Precursors (MPs) that each divide once to generate 2 neurons. MP1 generates the MP1 neurons, MP3 divides into H-cell and H-cell sib, and MP4-6 each divides into an iVUM/mVUM pair (iVUM4-6 and mVUM4-6) (Wheeler et al., 2008). A median neuroblast (MNB) generates ~8 embryonic neurons (MNB progeny; MNBp) and continues to divide post-embryonically (Truman and Bate, 1988; Wheeler et al., 2006). There are two distinct populations of midline glia (MG), the anterior midline glia (AMG) and posterior midline glia (PMG) (Dong and Jacobs, 1997; Wheeler et al., 2012; Wheeler et al., 2006). The PMG undergo apoptosis during late embryonic development and their function is unknown. Only a subset of the AMG survive, and they ensheath the axon commissures.

In addition to the cellular characterization of midline development, the molecular composition of the *Drosophila* CNS midline cells is well-defined. Previously, we analyzed the developmental distribution of 286 genes expressed in midline cells by in situ hybridization and immunostaining (Kearney et al., 2004; Wheeler et al., 2006). In addition, we analyzed the midline expression of 77 genes by confocal analysis, identifying the midline cell-type specificity of each during development (Wheeler et al., 2008; Wheeler et al., 2006). This data is accessible on the *Drosophila* CNS Midline Gene Expression Database (MidExDB; http://midline.bio.unc.edu;) (Wheeler et al., 2009b). Thus, each midline cell type can be identified at all stages of development, aiding in genetic analyses of midline cell development. Nevertheless, there has been relatively little characterization of the unique differentiated properties of each midline neuronal cell type, such as the presence and distribution of neuropeptides and neurotransmitter receptors.

In this paper, we use fluorescence activated cell sorting (FACS) to isolate midline cells at two major developmental periods and carry-out RNA-seq on each cell sample. The results were validated by comparison to the extensive knowledge of midline gene expression and by using in situ hybridization to verify midline expression of genes previously not known to be

expressed in midline cells. In this paper, we focus on the midline expression of neurotransmitters and their receptors. The data indicate that 9 neuropeptide precursor genes are expressed in subsets of CNS midline cells, including MP1 neurons, iVUMs, MNB progeny, and surprisingly, MG. In addition, 31 small-molecule neurotransmitter receptors and 13 neuropeptide receptor genes are expressed in a variety of midline cell types. In terms of the expression patterns of these genes, there exist both segmental differences and differences in specific iVUMs and MNB progeny. Among these results, the *short neuropeptide F precursor* (*sNPF*) gene is expressed in iVUM5, which has high levels of the Castor (Cas) transcription factor compared to iVUM4 and iVUM6. Genetic analyses demonstrate that *sNPF* expression in iVUM5 is absent in *cas* mutant embryos, while other differentiated properties of iVUM5 are unaffected. Thus, we propose a novel role of Cas in regulating *sNPF* neuropeptide gene expression. The combined use of FACS cell purification, RNA-seq analysis, in situ hybridization, and genetics allows the detailed analysis of how unique neurons acquire their differentiated state.

Materials and methods

Drosophila strains and genetics

3.7sim-Gal4 (Xiao et al., 1996) and *y¹ w**; *Pin^{Yt}*/*CyO*; P{*UAS-mCD8-GFP.L*}LL6 (Lee and Luo, 1999) were used to generate the *w^{1118}*; *3.7sim-Gal4; UAS-mCD8.GFP* strain (*3.7sim>mCD8.GFP*) used for cell sorting and in situ hybridization and immunostaining experiments. The *w^{1118}*; *3.7sim-Gal4 UAS-tau.GFP* strain (*3.7sim>tau.GFP*) (Brand, 1995; Wheeler et al., 2006) was also used for in situ hybridization and immunostaining experiments. *UAS-cas* strains (Kambadur et al., 1998) were provided by W. Odenwald (NINDS, Bethesda, MD), and the *cas^{24}* and *cas^{39}* mutant strains (Cui and Doe, 1992) were provided by C. Doe (University of Oregon, HHMI).

Collection and dissociation of embryos for cell sorting

3.7sim>mCD8.GFP flies were propagated at low density in 6 oz bottles with cornmeal-based food at 25°C. For embryo collections, recently eclosed flies were transferred to 900 cm^3 cages and acclimated for several days. Typically, 3 bottles were used to populate each cage, and 6–8 cages were used for each sample. On collection days, 100 mm grape agar plates with yeast paste were changed 3X for 2 hours/each to clear older embryos. Embryos were then collected for 2 hours on fresh yeasted grape agar plates and aged either 6–8 hours or 14–16 hours after egg laying (AEL) at 25°C. After staging, embryos were dechorionated with 100% bleach for 45 sec for 6–8 hour embryos or 1 min for 14–16 hour embryos, washed with 1X phosphate buffered saline (PBS) + 0.1% Tween-20, and placed on ice in 1X PBS. An aliquot of embryos was removed for immediate fixation and subsequent staging analysis. The remaining embryos were split into 1.5 ml microfuge tubes with ~25 µl packed embryos/tube. Generally, a total of 75–150 µl of packed embryos were used for each sample. PBS was removed and 100 µl of chilled dissociation buffer (9:1 10X Trypsin-EDTA:10X PBS) was added. Embryos were gently ground with a plastic pestle, and 400 µl of additional dissociation buffer was added. The cell solution was rocked on a nutator at room temperature for 10 min for 6–8 hour embryos and 20 min for 14–16 hour embryos. Cells were occasionally disrupted by pipetting. To terminate the trypsin digestion, tubes were placed on ice and 25 µl of heat-inactivated fetal bovine serum was added. Cells were filtered through a 41 µm nylon net into new microfuge tubes and 500 µl of chilled FACS buffer (1X PBS; 2% BSA; 2.5 mM EDTA) was added (FACS buffer was filtered through an 0.22 µm filter prior to use to remove particles that are detected by the flow cytometer). Cells were pelleted at 4°C for 4 min at $700 \times g$, washed with 500 µl chilled FACS buffer, pelleted, and resuspended in 200 µl of chilled FACS buffer. At this point, all tubes corresponding to a single embryo collection were combined, cells were filtered through a 41 µm nylon net,

counted on a hemacytometer, and diluted with chilled FACS buffer to a concentration of 10^6 cells/ml. Cells were kept on ice in the dark until sorted.

Cell sorting and cDNA library preparation

Cell sorting was performed on the same day as the embryo dissociation. Prior to sorting, propidium iodide was added to a final concentration of 1 μg/ml. Cells were sorted into populations of GFP^{+} midline cells and GFP[−] non-midline cells on a Sony/iCyt Reflection cell sorter at the Flow Cytometry Core Facility (http://flowcytometry.med.unc.edu) at UNC Chapel Hill School of Medicine. Cell sorting was based on forward scatter and back scatter properties, the presence or absence of propidium iodide fluorescence to exclude dead or ruptured cells, and GFP fluorescence intensity. Cells were sorted directly into RNeasy Mini Kit Lysis Buffer (Qiagen) and frozen in a dry ice/ethanol bath. Before and after the main sort, an aliquot of cells were sorted into PBS and analyzed in the flow cytometer to estimate the accuracy of sorting.

Total RNA was prepared using the RNeasy Mini Kit, treated with RNase-free DNase (Qiagen), and re-purified with the RNeasy Mini Kit. mRNA was isolated using the Poly(A)Purist MAG Kit (Ambion), fragmented at 70°C for exactly 2 min with 10X Fragmentation Reagent (Ambion), and precipitated. First-strand cDNA was generated with SuperScript III Reverse Transcriptase (Invitrogen) using random hexamers. Second-strand cDNA was generated and purified according to the "mRNA Sequencing, Sample Preparation Guide" (Illumina; Rev. D, Sept. 2009) using 5X Second Strand Buffer (Invitrogen), DNA polymerase I (New England BioLabs; NEB), and the QIAquick PCR Purification Kit (Qiagen). End repair of cDNA fragments, adenylation of 3′ ends, and ligation of adapters were performed as described in "Preparing Samples for Sequencing Genomic DNA/Chip-Seq (v2.5)" provided by the UNC High-Throughput Sequencing Facility (HTSF). Adapters were obtained from the HTSF, and all other reagents were obtained from NEB. Purification of samples between steps was done using Qiagen kits as described in the Illumina protocol mentioned above. Adapter-ligated cDNA fragments (200–300 bp in length) were purified from a 2% agarose gel using the QIAquick Gel Extraction Kit. The adapter-ligated fragments were enriched with 18 cycles of PCR using Phusion High-Fidelity DNA polymerase (NEB) with primers obtained from the HTSF. The generated cDNA library was purified with the QIAquick PCR Purification Kit and sequenced on an Illumina GAIIx at the HTSF to generate single-ended 76 nucleotide reads.

Alignment of high-throughput sequencing reads

From the Illumina-generated fastq files, sequence reads were aligned to the *D. melanogaster* genome (build 5) using Bowtie (version 0.12.7) and TopHat (version 1.3.1.OSX_x86_64) with the following non-default parameters: -i 20 -I 142000 -g 1 --solexa1.3-quals (Langmead et al., 2009; Trapnell et al., 2009). The chosen minimum (-i) and maximum (-I) allowable intron lengths were based on known, annotated intron lengths in the *D. melanogaster* genome as reported on FlyBase (McQuilton et al., 2012). Only reads mapping uniquely to the genome were considered (-g 1). Cufflinks (version 1.0.3.OSX_x86_64) was run with the *D. melanogaster* reference annotation r5.39 to associate mapped reads with genes and calculate expression values (Trapnell et al., 2010). A mask file was used to eliminate the mapping of reads to rRNA, tRNA, snRNA, snoRNA, snmRNA, and ribosomal protein genes during this process.

All samples were processed individually; however, the two CNS midline samples from each time-point were also processed together in TopHat as replicates (Table 1). In the analyses that follow, a gene was considered to be expressed in the CNS midline cells above a certain threshold value if the following two conditions were met: (1) The average of the individual

FPKM values (Fragments Per Kilobase of exon per Million fragments mapped) for that gene from both CNS midline samples was above the threshold value. (2) The FPKM value for that gene when the two CNS midline samples were processed as replicates was above the threshold value. All CNS midline expression values reported here are the FPKM values obtained when the two CNS midline samples were processed as replicates.

In situ hybridization and immunostaining

Standard protocols for alkaline phosphatase and fluorescent in situ hybridization, and immunostaining were previously described (Kearney et al., 2004). These protocols are available on MidExDB (http://midline.bio.unc.edu/MDB_Display_protocols.aspx). For in situ hybridization experiments, digoxigenin or biotin-labeled RNA probes were generated from cDNA clones in the *Drosophila* Gene Collection Releases 1 and 2 (Berkeley *Drosophila* Genome Project) or from cDNA amplicons generated using a 3′ primer containing a T3 RNA polymerase binding site (Supplemental Tables S1, S2). RNA detection was carried-out using anti-digoxigenin-AP Fab fragments (Roche), anti-Digoxigenin-POD Fab fragments (Roche), streptavidin-HRP (PerkinElmer), and the Tyramide Signal Amplification (TSA) system (PerkinElmer). For immunostaining, the primary antibodies used were: rabbit anti-GFP (Abcam), mouse anti-Tau (Sigma-Aldrich), rabbit anti-Cas (W. Odenwald, NINDS) (Kambadur et al., 1998), guinea pig anti-Zfh1 (Fortini et al., 1991), and mouse anti-En (4D9; Developmental Studies Hybridoma Bank). Secondary antibodies were conjugated with Alexa Fluor dyes (Invitrogen).

Data distribution

Raw sequencing read files and Cufflinks processed genes.fpkm_tracking files have been deposited in the Gene Expression Omnibus (GEO) at the National Center for Biotechnology Information (NCBI). FPKM values of genes are also accessible on MidExDB (http://midline.bio.unc.edu).

Results

Isolation of fluorescently-labeled CNS midline cells

To further understand the development and differentiated properties of *Drosophila* embryonic midline neurons and glia, we used RNA-seq to determine the midline cell transcriptome. The protocol involved using FACS isolation of GFP-labeled embryonic midline cells, followed by mRNA isolation and RNA-seq analysis. High-quality, biologically-relevant results require careful attention to multiple criteria. (1) Midline cell expression of the fluorescent marker (GFP) must be sufficiently strong for the cell sorter to distinguish labeled cells from unlabeled cells. (2) There should be minimal expression of the fluorescent marker outside of the CNS midline. (3) Fluorescent marker expression must be consistently strong in all midline cells throughout the developmental periods analyzed. (4) Expression of the transgenic marker should have no adverse effects on embryonic development. Multiple *Gal4* and UAS lines were analyzed, and a *3.7sim-Gal4; UAS-mCD8.GFP* (*3.7sim>mCD8.GFP*) strain best matched the criteria described above. This strain uses the early midline enhancer from the *single-minded* (*sim*) gene (Nambu et al., 1991; Xiao et al., 1996), which encodes a bHLH-PAS protein and is a master regulator of CNS midline gene expression (Nambu et al., 1991).

The two embryonic developmental time-points selected for this study were: (1) 6–8 hours after egg laying (AEL) (stages 11–12), which represents a time when the CNS midline neurons have recently arisen from their precursors and are acquiring their respective cell identities and beginning to differentiate, and (2) 14–16 hours AEL (stages 16–17), a time in which CNS midline neurons and glia are well-differentiated (Wheeler et al., 2008; Wheeler

et al., 2006). Staining *3.7sim>mCD8.GFP* embryos with anti-GFP revealed that embryos had strong and specific GFP expression in all CNS midline cells at both 6–8 hours and 14–16 hours AEL (Fig. 1A–D). Furthermore, >99% of *3.7sim>mCD8.GFP* embryos aged 6–8 hours and 14–16 hours AEL were at the proper stages of development.

Dissociated embryonic cells were FACS-sorted into populations of GFP+ CNS midline cells and GFP− non-midline cells (Fig. 1E,F). GFP+ midline cells were successfully sorted with >95% purity, based on pre- and post-sorting checks of accuracy on the flow cytometer (Fig. 1G). Two independently-collected CNS midline samples and one non-midline sample were analyzed for each time-point (Table 1).

mRNA sequencing and data validation

For each of the sorted cell samples, mRNA was isolated and sequenced on an Illumina GAIIx. Single-ended 76 nucleotide reads were generated, and analyses with FastQC software indicated high quality reads (Fig. 1H,I). Uniquely mapping reads were aligned to the annotated *D. melanogaster* genome using the Bowtie, TopHat, and Cufflinks programs (Langmead et al., 2009; Trapnell et al., 2010; Trapnell et al., 2009).

Surveying well-characterized genes with no known midline expression indicated that these genes had FPKM (Fragments Per Kilobase of exon per Million fragments mapped) values <5 in the CNS midline RNA-seq data (Supplemental Table S3). These genes include those expressed in the lateral CNS, sensory cells, midline accessory cells (channel glia, dorsal median cells), muscle, and trachea. Previous studies have characterized the CNS midline cell-type specific expression of 77 genes by confocal microscopy (Wheeler et al., 2009a; Wheeler et al., 2006). To initially validate the fidelity of the midline RNA-seq data, the FPKM values for these midline-expressed genes were assessed. Of the 77 genes, 75 are expressed between stages 11–17, the time-points used in our experiments. All 75 of these genes had an FPKM value >5 in either the 6–8 hour or 14–16 hour samples (or both) (Supplemental Table S4). Thus, we designate genes with a midline FPKM value 5 as "expressed" in midline cells, and an FPKM value <5 as "not expressed, or expressed at a low level." This MidExDB data set included genes that are expressed in a single midline cell type. Since these genes often showed high midline FPKM values in the RNA-seq data, these results further confirm the sensitivity of the RNA-seq data and that all cell types were present in the sorted CNS midline samples.

RNA-seq data predicts CNS midline gene expression

To test the predictive abilities of the RNA-seq data, we addressed whether these data could identify factors that are enriched in the midline cells. To concentrate on transcription factors and transcriptional regulators, we first generated a list of 859 genes that contain the term "transcription" in their FlyBase gene ontology entries. We find that 508 of these genes are expressed in the 14–16 hour midline sample with FPKM values 5 and 292 with FPKM values 20. We then searched this list for genes with FPKM values 20 in the 14–16 hour midline sample and <5 in the 14–16 hour non-midline sample, reasoning that a 4-fold difference of FPKM values will identify genes with strong midline expression and relatively low expression outside the midline when analyzed by in situ hybridization. This search identified 6 genes: *cryptochrome* (*cry*), *doublesex-Mab related 99B* (*dmrt99B*), *HLH3B*, *period* (*per*), *sim*, and *vestigial* (*vg*) (Fig. 2A) (note that *Drosophila cry* encodes a blue light photoreceptor, and is not a transcription factor in *Drosophila*). Analysis in vivo by in situ hybridization confirmed that the expression of all 5 genes, in addition to *sim*, is highly enriched in the CNS midline (Fig. 2C–G). These genes were further analyzed for midline cell expression using fluorescent in situ hybridization in combination with midline cell type-specific markers (Fig. 2B). The two circadian rhythm-associated genes, *cry* and *per*, show

expression in non-overlapping midline neurons. Expression of the *cry* gene colocalizes with the MP1 neuron marker *odd skipped* (*odd*) (Fig. 2H), whereas *per* expression is specific to H-cell sib, iVUM4-6, and the MNBp, as previously shown for a *per-Gal4* transgenic strain (Wheeler et al., 2006). Transcripts for *dmrt99B* and *vg* both colocalize with Zinc finger homeodomain 1 (Zfh1) protein, indicating expression in the 3 mVUM motoneurons (Fig. 2I,J) (Guss et al., 2008). Expression of *HLH3B* was observed in Engrailed (En)[+] iVUMs (Fig. 2K) and H-cell sib, which has high levels of *Vesicular glutamate transporter* (*VGlut*) expression (data not shown). Thus, the ability of the RNA-seq and in situ hybridization data to identify transcriptional regulatory genes with high midline specificity expands the list of known transcription factors that may control midline neuron-specific gene expression.

Quantitative analysis of the CNS midline transcriptome

The examination of the midline RNA-seq data indicated that both 6–8 hour and 14–16 hour midline samples are a valid representation of the midline transcriptome, allowing a quantitative assessment of midline transcription during those two time periods. At the time of these experiments, there were 13909 protein coding genes annotated for *D. melanogaster* (McQuilton et al., 2012). When examining genes for which reliable RNA-seq data were obtained for both time-points, we see 6094 genes expressed in the CNS midline at 6–8 hours AEL with FPKM values   5, and 6529 genes at 14–16 hours AEL. Of these genes, 5041 (66.5%) were expressed at both time-points with 2541 genes (33.5%) expressed in only one time interval (Fig. 2L). The large difference in gene expression between the 2 stages reflects the rapid changes in development that occur as the cells transition from a group of cells at stages 11–12 that are undergoing dramatic changes in cell fate, migration, and apoptosis to differentiated neurons and glia (stages 16–17). Comparing CNS midline to non-midline gene expression, we find that at either time-point, most genes (79–84%) expressed with FPKM values   5 are shared between the 2 samples, while only 4–6% of genes are specific to the CNS midline cells (Fig. 2M,N). Not surprisingly, more genes (10–17%) are expressed only in non-midline cells compared to those only expressed in midline cells.

CNS midline neurons utilize a diverse array of neuropeptides

The CNS midline neurons have been well-characterized with respect to the neurotransmitters they utilize: MP1 neurons (Pigment-dispersing factor (Pdf) and Proctolin (Proct)), H-cell (dopamine), H-cell sib (glutamate), iVUMs (GABA), and mVUMs (glutamate, octopamine) (Wheeler et al., 2006). Consistent with these assignments, the RNA-seq data generally showed high levels of expression for genes involved in the generation, metabolism, and transport of these neurotransmitters (data not shown). The RNA-seq data was further screened for the utilization of additional neurotransmitters. None of the midline neurons are likely to utilize acetylcholine, histamine, or serotonin, based on a lack of expression of *Choline acetyltransferase* (FPKM=3.76), *Histidine decarboxylase* (FPKM=0.79), or *Serotonin transporter* (FPKM=2.62). However, analysis of 33 *Drosophila* neuropeptide precursor genes in the 14–16 hour RNA-seq data revealed that 12 of these genes have FPKM values   5, including *Pdf* and *Proct* (Fig. 3A,B). Here, we characterize the expression of the remaining 10 neuropeptide precursor genes in midline segments S1-A7, and arrange their expression by cell type (Fig. 3L).

MP1 neurons—The *Neuropeptide-like precursor 1* (*Nplp1*) gene is expressed in *odd*^{+} MP1 neurons in all segments (Fig. 3C). Along with *Pdf* and *Proct*, this increases the number of neuropeptide genes expressed in MP1 neurons to three. The MP1 neurons undergo apoptosis in segments S3-A4 at late embryogenesis (Miguel-Aliaga and Thor, 2004). In larval segments A8/9, the MP1s likely innervate the hindgut, suggesting that Pdf, Proct, and Nplp1 peptides may regulate hindgut activity.

iVUM neurons—Four neuropeptide precursor genes are expressed in subsets of the GABAergic iVUM interneurons. iVUMs are local interneurons of unknown function. *Myoinhibiting peptide precursor* (*Mip*), which has been implicated in ecdysis in *Drosophila* and inhibiting ecdysteroid synthesis in other insects (Kim et al., 2006; Veelaert et al., 1996), is expressed in only 1 En$^-$ cell of segment S1 and 1 cell of segment S3. While the lineages of the suboesophageal midline cells have not been characterized in detail, the *Mip*$^+$ cell in segment S3 is En$^+$ Cas^{lo}, indicative of iVUM4 neurons (Fig. 3D). The diuretic hormone precursor genes *Dh31* and *Dh44*, are also expressed in iVUM neurons. Diuretic hormone peptides are implicated in peristalsis and in controlling water and ion balance by acting on the Malpighian tubules (Cabrero et al., 2002; Coast et al., 2001; LaJeunesse et al., 2010). *Dh44* is expressed in iVUM6 (En$^+$ Cas$^-$) of segments A2-A5 and an En$^+$ Cas$^-$ cell of segment S3 (Fig. 3E), while *Dh31* is expressed in iVUM5 (En$^+$ Cas^{hi}) of segment A7 and an En$^-$ Cas$^+$ cell of segments S1 and S2 (Fig. 3F). The *short neuropeptide F precursor* (*sNPF*) gene, which encodes peptides involved in feeding behavior (Lee et al., 2004), is expressed in iVUM5 (En$^+$ Cas^{hi}) of segments S3-A7, and an En$^+$ cell of segment S1 (Fig. 3G). These results revealed several novel findings. (1) The GABAergic iVUM interneurons likely utilize a variety of neuropeptides in neurotransmission. (2) Each neuropeptide is expressed only in a specific iVUM – either iVUM4, iVUM5, or iVUM6. This indicates that each iVUM is distinct physiologically, despite their general similarities in gene expression and axonogenesis. (3) There exist segmental differences in the embryonic expression of each neuropeptide with the most extreme case being *Mip*, which is only expressed in segments S1 and S3, indicating there are functional differences between iVUM neurons of different segments. It remains possible that expression of these neuropeptide genes may emerge in additional segments later in development, but even so, there would still exist segmental differences in neuropeptide gene appearance.

MNB progeny—In segments S3-T3, we observed *Nplp1* expression in 2 En$^-$ MNBp (Fig. 3H). Expression of *Leucokinin* (*Lk*), which has been implicated in regulating diuresis and meal size (Al-Anzi et al., 2010; Terhzaz et al., 1999), is present in a single En$^+$ MNBp in segments S3-A7 (Fig. 3I).

MG—In *Drosophila*, the neuropeptide *ion transport peptide* (*itp*) is expressed in dorsal and ventral lateral clock neurons (Dircksen et al., 2008; Johard et al., 2009). While its function in these neurons is unknown; in locusts, Itp has been shown to play an antidiuretic role, involved in the reabsorption of ions and fluids in the hindgut (Audsley et al., 1992; King et al., 1999). Interestingly, in the CNS midline, *itp* is not expressed in neurons, but in MG (Fig. 3J). Expression was present in AMG, but not PMG, in all segments.

Non-midline RNA-seq$^+$ genes—Three neuropeptide precursor genes, *bursicon* (*burs*), *Neuropeptide-like precursor 2* (*Nplp2*), and *Adipokinetic hormone* (*Akh*) were not detected by in situ hybridization in CNS midline cells, yet were present in the 14–16 hour midline RNA-seq data with FPKM values 5. The 3′ end of the coding sequence of the *burs* gene is 139 bp downstream of the annotated 3′-UTR of the *GABA-B-R2* gene, which has an FPKM value of 87.69 in the 14–16 hour midline sample (Table 2). One possibility is that the 3′-UTR of *GABA-B-R2* may overlap the *burs* gene leading to *burs* being scored as midline-expressed. Expression of *Nplp2* is observed in hemocytes that are also GFP$^+$ (Fig. 3K). During embryogenesis, ~70% of MG undergo apoptosis and are engulfed by hemocytes (Sonnenfeld and Jacobs, 1995; Wheeler et al., 2012). Consequently, hemocytes that engulf GFP$^+$ MG will be FACS-sorted into the GFP$^+$ sample, explaining the occurrence of high *Nplp2* FPKM values. For *Akh*, the obtained FPKM value is 5.34, just above the threshold for considering a gene as "expressed" in the midline, and it likely represents a false-positive.

Neuropeptide receptors are expressed in diverse CNS midline neuronal cell types

Previous work has identified a variety of neurotransmitter receptor genes expressed in midline neurons, including *Glu-RI*, *5-HT1A*, and *NPFR1* (Wheeler et al., 2006). We have utilized the midline 14–16 hour RNA-seq data to further characterize neurotransmitter receptor expression in midline cells. Of 38 neurotransmitter receptors genes analyzed, 31 have midline FPKM values 5 at 14–16 hours AEL (Table 2), including *Glu-RI* and *5-HT1A*. This suggests that the midline cells are able to respond to a wide variety of neural inputs. Complementing this analysis, we also analyzed the expression of 19 *Drosophila* neuropeptide receptors and found that 13 have 14–16 hour midline FPKM values 5, including *NPFR1* (Fig. 4A,B). Using in situ hybridization, we further investigated their expression in segments T1-A7.

Motoneurons—The *CCHamide-1 receptor* (*CCHa1r*) and *short neuropeptide F receptor* (*sNPF-R*) genes are both expressed in MP1 and mVUM motoneurons (Fig. 4C–F). *Drosophila* sNPF is implicated in appetite control and food uptake (Lee et al., 2004), and presence of the sNPF receptor on MP1s and all 3 mVUMs links feeding behavior to midline-controlled gut peristalsis (MP1s) and locomotion (mVUMs). The *CCHamide-2 receptor* (*CCHa2r*) is also expressed in mVUMs, although its expression is restricted to abdominal segments and is highest in the posterior-most mVUM6 neurons (Fig. 4G). The *Fmrf Receptor* (*FR*) is expressed in all 3 mVUM neurons of segments T3-A7 (Fig. 4H).

Interneurons—Midline interneurons also express a variety of neuropeptide receptors. Expression of *FR* is segmentally restricted in several interneurons, with expression seen in iVUM4 neurons of segments T1–T2 and H-cell neurons of segments T1-A1 (Fig. 4I; data not shown). *Cardioacceleratory peptide receptor* (*CcapR*) showed the most restricted expression domain in the CNS midline of all neuropeptide receptors examined, with expression present in iVUM4 neurons of segments A5–A7 (Fig. 4J). The diuretic hormone receptor genes *Dh31-R1* and *Dh44-R1*, have overlapping midline expression patterns, with both present in H-cell and H-cell sib (Fig. 4K–N). The Dromyosuppressin receptor genes *DmsR-1* and *DmsR-2* show overlapping patterns of expression in iVUM4 and iVUM6, but not iVUM5 (Fig. 4O,P).

Broad expression—Three hormone receptor genes are broadly expressed in the CNS midline neurons. The Tachykinin-like receptor genes *Takr86C* and *Takr99D* are expressed in most midline neurons (Fig. 4Q,R), with *Takr99D* expressed at highest levels in an En[+] MNBp. *Ecdysis-triggering hormone receptor* (*ETHR*) is the most broadly expressed of the neuropeptide receptors, with expression in all midline neurons and MG (data not shown). *ETHR* has two splice variants, *ETHR-RA* and *RB*, (Iversen et al., 2002). Our 14–16 hour midline RNA-seq data show both variants expressed at roughly equal levels (FPKM values of 4.3 and 3.2 for RA and RB, respectively), similar to the whole animal RNA-Seq data (Graveley et al., 2011).

Castor is a positive regulator of sNPF expression in iVUM5

The ability to assign expression profiles for each neuropeptide and neurotransmitter receptor to specific midline cells facilitates the genetic analysis of their regulation. The most interesting aspect of *sNPF* expression is that it is present in only iVUM5 and not iVUM4 or iVUM6. While most characterized transcription factors are expressed in all 3 iVUMs, levels of the Castor (Cas) zinc finger transcription factor protein vary for each iVUM: being low in iVUM4, high in iVUM5, and absent in iVUM6 (Fig. 5A) (Wheeler et al., 2008). The high levels of Cas in iVUM5 suggest that it might control *sNPF* expression. Examining two *castor* protein-null alleles, *cas[24]* and *cas[39]*, there was a complete absence of iVUM5-specific *sNPF* expression in both homozygous and *trans*-heterozygous mutant embryos (Fig. 5B,C).

This effect is specific to the midline, since non-midline CNS expression of *sNPF* is present in *cas* mutant embryos (Fig. 5B′,C′). In general, midline neurons and glia are present in *cas* mutants, indicating no gross disorganization. More specifically, expression of *en* and *Glutamic acid decarboxylase 1* (*Gad1*) is unaffected in *cas* mutant embryos in all 3 iVUMs (Fig. 5F–I). This is consistent with iVUM neurons being properly specified and undergoing differentiation to become GABAergic in the *cas* mutants. Therefore, the defect in iVUM5 neuronal differentiation in *cas* mutants is limited to the loss of *sNPF* expression for the genes analyzed.

Misexpression of high levels of *cas* in all midline neurons and glia in *3.7sim-Gal4 UAS-cas* embryos did not result in ectopic *sNPF* expression (Fig. 5D), indicating that other factors, in addition to high levels of Cas, are necessary for *sNPF* expression. Supporting this hypothesis, midline misexpression of *cas* (*3.7sim-Gal4 UAS-cas*) in *cas* mutants completely rescues expression of *sNPF* in only a single cell per midline segment (Fig. 5E). One model that would explain these observations includes a transcriptional activator that is present in iVUM5, but absent from iVUM4 and iVUM6. In this model, both Cas and a second coactivator are necessary for *sNPF* expression. A second model proposes the presence of a transcriptional repressor in iVUM4 and iVUM6. This repressor would keep *sNPF* expression off in these cells, even when *cas* is misexpressed at high levels. The *cas* gene also controls development of the *Drosophila Lk*, *FMRFa*, *Nplp1*, and *Capa* peptidergic neurons (Benito-Sipos et al., 2010; Gabilondo et al., 2011; Losada-Pérez et al., 2010). However, in those cases, it is proposed that *cas* is acting as a temporal identity gene required for neuronal cell fate, whereas in iVUM5, we propose that *cas* does not direct neuronal cell fate, but influences differentiation – specifically neuropeptide expression.

Discussion

In this paper, we have combined the use of FACS purification of midline cells, RNA-seq, and in situ hybridization to study the differentiation of midline neurons. Based on this data, we have defined a midline-expressed gene as having an FPKM ≥ 5 in the midline GPF+ samples. Examining the RNA-seq data for expression values of 75 genes known to be expressed in midline cells, we found that all 75 had an FPKM > 5 (5.30 – 1351.15). Similarly, we examined 24 genes that are not thought to be expressed in midline cells, and they all had an FPKM < 5 (0.00 – 4.98). As a test of our RNA-seq data, we used fluorescent in situ hybridization to examine the expression of 22 neuropeptide precursor and neuropeptide receptor genes with FPKM values > 5 (5.34 – 1058). Of the 22 genes tested, 19 had midline expression. Of the three genes that had undetectable midline expression, one was expressed in hemocytes and was likely detected because they had engulfed a GFP+ midline cell, one may represent an annotation error due to proximity to a midline–expressed gene, and the other had an FPKM just barely above our threshold of 5. Thus, the false negative rate from our analyses is 0% (0/75) and the false positive rate is <14% (3/22). Consequently, the RNA-seq data and our threshold designations are strong indicators of midline expression.

The expression of neuropeptide precursor genes in a variety of midline neurons indicate that these neurons commonly co-utilize small molecule and peptide neurotransmitters. The 3 iVUMs are GABAergic interneurons with similar axonal trajectories. We showed that iVUM4 expresses *Mip*, iVUM5 expresses *sNPF* (plus *Dh31* in segment A7), and iVUM6 expresses *Dh44*. Thus, despite near identity in their previously studied gene expression, iVUM4, iVUM5, and iVUM6 possess differences in gene expression and in their likely modes of neurotransmission. These results also indicate that iVUMs are peptidergic in addition to utilizing GABA as a neurotransmitter. Co-transmission of neuropeptides with small-molecule neurotransmitters has been documented in both vertebrates and invertebrates

(Hökfelt et al., 2000; Burnstock, 2004; Nässel and Homberg, 2006). Recent work on the *Drosophila* brain central complex has described *FMRFamide-related (Fmrf)* neuropeptide gene expression in GABAergic neurons, *Mip* and *Tachykinin* (*Tk*) expression in cholinergic neurons, and *sNPF* expression in both cholinergic and glutamatergic neurons (Kahsai and Winther, 2011). In the case of iVUMs, it needs to be demonstrated that these cells generate neuropeptides that play functionally relevant roles in neurotransmission.

One unexpected observation is that midline expression of *itp* is present in MG, but absent in neurons. Neuropeptide expression in glia is observed in vertebrate systems and has been implicated in processes like axon guidance, neuronal survival, neuronal proliferation, and immunity (Ubink et al., 2003). To our knowledge, this is the first reported case in *Drosophila* of glial neuropeptide expression. Since MG are in close apposition to commissural axons (e.g. Wheeler et al., 2009a), as well as extend laterally through gliopodia (Vasenkova et al., 2006), it is possible that MG may be modulating neurotransmission, or playing some other developmental, physiological, or homeostatic role.

It is important to note that our expression analysis is relegated to late stage embryos, and that the patterns of expression may differ in larvae and adults. In fact, comparing our embryonic midline expression data to the comprehensive analysis of neuropeptide distribution in 3rd instar larvae (Park et al., 2008) reveals significant differences for most of the genes analyzed. In the larvae, there are no detectable levels of DH44, ITP, LK, NPLP1, or sNPF in midline cells, and even though DH31, PDF, and PROCT may be present in midline cells, their distribution is more restricted than embryonic precursor gene expression. It will be informative to examine neuropeptide appearance in 1st instar larvae to see whether the neuropeptide distribution fits with embryonic expression of the precursor genes. If so, this would indicate significant changes in neuropeptide gene expression during larval development. Alternatively, the 3rd instar levels of neuropeptide may be present in midline cells reflecting embryonic precursor gene expression, but too low to clearly detect. In many large neurosecretory cells of the nervous system, the bHLH transcription factor Dimmed (Dimm) acts as a scaling factor that up-regulates genes involved in neurosecretion (Mills and Taghert, 2012). Our RNA-seq data suggest that *dimm* is not highly expressed in the peptidergic neurons of the CNS midline cells at stages 16–17 (FPKM <5), consistent with the lack of anti-Dimm immunostaining in embryonic midline cells (Park et al., 2008), except in Pdf+ neurons in segment A8/9. This suggests that neuropeptide production in midline neurons may be relatively low, possibly reflecting differences in function from high-producing neurons.

Small-molecule neurotransmitter receptor expression is diverse in midline neurons, with 31 receptor genes expressed with FPKM values >5. These include inputs for acetylcholine, dopamine, GABA, glutamate, octopamine, and serotonin. Additionally, 13 neuropeptide receptors are expressed in subsets of midline cells. Interestingly, there are several examples where midline neurons secrete specific neuropeptides, and different midline neurons possess their receptors. For example, *Dh31-R1* and *Dh44-R1* are expressed in H-cell and H-cell sib, and iVUM5 and iVUM6 neuron express *Dh31* and *Dh44*, respectively. In addition, iVUM5 expresses *sNPF* while the MP1 neurons and mVUMs express *sNPF-R*. However, at this time, it is unknown whether the midline-directed neurosecretion directly influences midline neurotransmission.

Using data obtained from our RNA-seq experiments with information already known about CNS midline cell gene expression, we were also able to link the activity of a transcription factor with neuropeptide expression. The role of Cas as a temporal identity factor important during the specification of lateral CNS cells has been well established (Grosskortenhaus et al., 2006; Isshiki et al., 2001). In the CNS midline cells, we found that *cas* does not specify

the neurons it is expressed in, but is required in iVUM5 neurons for the expression of the *sNPF* neuropeptide gene. Our observation that *cas* is not sufficient to drive *sNPF* expression in other CNS midline cells, including iVUM4 and iVUM6, suggests that other iVUM5-specific factors are required in addition to *cas*. Since *cas* affects iVUM5 *sNPF* expression, but not that of *Gad1*, this indicates that multiple regulatory proteins control different aspects of iVUM5 differentiation. This contrasts with the general view of neuronal differentiation in *C. elegans* in which neuronal differentiation is largely co-regulated (e.g. Kratsios et al., 2012; Hobert, 2011). This manuscript has focused on only a small fraction of the midline RNA-seq data, and future analyses of the data will be likely reveal additional insight into the regulation of neural and glial differentiation. One important extension of this approach will be to purify subsets of CNS midline neurons and glia followed by RNA-seq analysis to assess the similarities and differences of individual midline cell types.

Supplementary Material

Refer to Web version on PubMed Central for supplementary material.

Acknowledgments

References

Al-Anzi B, Armand E, Nagamei P, Olszewski M, Sapin V, Waters C, Zinn K, Wyman RJ, Benzer S. The leucokinin pathway and its neurons regulate meal size in *Drosophila*. Curr Biol. 2010; 20:969–978. [PubMed: 20493701]

Audsley N, McIntosh C, Phillips JE. Isolation of a neuropeptide from locust corpus cardiacum which influences ileal transport. J Exp Biol. 1992; 173:261–274. [PubMed: 1487715]

Benito-Sipos J, Estacio-Gómez A, Moris-Sanz M, Baumgardt M, Thor S, Díaz-Benjumea FJ. A genetic cascade involving *klumpfuss*, *nab* and *castor* specifies the abdominal leucokinergic neurons in the *Drosophila* CNS. Development. 2010; 137:3327–3336. [PubMed: 20823069]

Brand A. GFP in *Drosophila*. Trends Genet. 1995; 11:324–325. [PubMed: 8585131]

Burnstock G. Cotransmission. Curr Opin Pharmacol. 2004; 4:47–52. [PubMed: 15018838]

Cabrero P, Radford JC, Broderick KE, Costes L, Veenstra JA, Spana EP, Davies SA, Dow JA. The *Dh* gene of *Drosophila melanogaster* encodes a diuretic peptide that acts through cyclic AMP. J Exp Biol. 2002; 205:3799–3807. [PubMed: 12432004]

Coast GM, Webster SG, Schegg KM, Tobe SS, Schooley DA. The *Drosophila melanogaster* homologue of an insect calcitonin-like diuretic peptide stimulates V-ATPase activity in fruit fly Malpighian tubules. J Exp Biol. 2001; 204:1795–1804. [PubMed: 11316500]

Cui X, Doe CQ. *ming* is expressed in neuroblast sublineages and regulates gene expression in the *Drosophila* central nervous system. Development. 1992; 116:943–952. [PubMed: 1339340]

Dircksen H, Tesfai LK, Albus C, Nässel DR. Ion transport peptide splice forms in central and peripheral neurons throughout postembryogenesis of *Drosophila melanogaster*. J Comp Neurol. 2008; 509:23–41. [PubMed: 18418898]

Dong R, Jacobs JR. Origin and differentiation of supernumerary midline glia in *Drosophila* embryos deficient for apoptosis. Dev Biol. 1997; 190:165–177. [PubMed: 9344536]

Fortini ME, Lai ZC, Rubin GM. The *Drosophila zfh-1* and *zfh-2* genes encode novel proteins containing both zinc-finger and homeodomain motifs. Mech Dev. 1991; 34:113–122. [PubMed: 1680376]

Gabilondo H, Losada-Pérez M, Del Saz D, Molina I, León Y, Canal I, Torroja L, Benito-Sipos J. A targeted genetic screen identifies crucial players in the specification of the *Drosophila* abdominal Capaergic neurons. Mech Dev. 2011; 128:208–221. [PubMed: 21236339]

Graveley BR, Brooks AN, Carlson JW, Duff MO, Landolin JM, Yang L, Artieri CG, van Baren MJ, Boley N, Booth BW, Brown JB, Cherbas L, Davis CA, Dobin A, Li R, Lin W, Malone JH, Mattiuzzo NR, Miller D, Sturgill D, Tuch BB, Zaleski C, Zhang D, Blanchette M, Dudoit S, Eads B, Green RE, Hammonds A, Jiang L, Kapranov P, Langton L, Perrimon N, Sandler JE, Wan KH, Willingham A, Zhang Y, Zou Y, Andrews J, Bickel PJ, Brenner SE, Brent MR, Cherbas P, Gingeras TR, Hoskins RA, Kaufman TC, Oliver B, Celniker SE. The developmental transcriptome of *Drosophila melanogaster*. Nature. 2011; 471:473–479. [PubMed: 21179090]

Grosskortenhaus R, Robinson KJ, Doe CQ. Pdm and Castor specify late-born motor neuron identity in the NB7-1 lineage. Genes Dev. 2006; 20:2618–2627. [PubMed: 16980589]

Guss KA, Mistry H, Skeath JB. *Vestigial* expression in the *Drosophila* embryonic central nervous system. Dev Dyn. 2008; 237:2483–2489. [PubMed: 18697219]

Hobert O. Regulation of terminal differentiation programs in the nervous system. Annu Rev Cell Dev Biol. 2011; 27:681–696. [PubMed: 21985672]

Hökfelt T, Broberger C, Xu ZQ, Sergeyev V, Ubink R, Diez M. Neuropeptides--an overview. Neuropharmacology. 2000; 39:1337–1356. [PubMed: 10818251]

Isshiki T, Pearson B, Holbrook S, Doe CQ. *Drosophila* neuroblasts sequentially express transcription factors which specify the temporal identity of their neuronal progeny. Cell. 2001; 106:511–521. [PubMed: 11525736]

Iversen A, Cazzamali G, Williamson M, Hauser F, Grimmelikhuijzen CJ. Molecular identification of the first insect ecdysis triggering hormone receptors. Biochem Biophys Res Commun. 2002; 299:924–931. [PubMed: 12470668]

Johard HA, Yoishii T, Dircksen H, Cusumano P, Rouyer F, Helfrich-Förster C, Nässel DR. Peptidergic clock neurons in *Drosophila*: ion transport peptide and short neuropeptide F in subsets of dorsal and ventral lateral neurons. J Comp Neurol. 2009; 516:59–73. [PubMed: 19565664]

Kahsai L, Winther ÅM. Chemical neuroanatomy of the *Drosophila* central complex: distribution of multiple neuropeptides in relation to neurotransmitters. J Comp Neurol. 2011; 519:290–315. [PubMed: 21165976]

Kambadur R, Koizumi K, Stivers C, Nagle J, Poole SJ, Odenwald WF. Regulation of POU genes by *castor* and *hunchback* establishes layered compartments in the *Drosophila* CNS. Genes Dev. 1998; 12:246–260. [PubMed: 9436984]

Kearney JB, Wheeler SR, Estes P, Parente B, Crews ST. Gene expression profiling of the developing *Drosophila* CNS midline cells. Dev Biol. 2004; 275:473–92. [PubMed: 15501232]

Kim YJ, Zitnan D, Galizia CG, Cho KH, Adams ME. A command chemical triggers an innate behavior by sequential activation of multiple peptidergic ensembles. Curr Biol. 2006; 16:1395–1407. [PubMed: 16860738]

King DS, Meredith J, Wang YJ, Phillips JE. Biological actions of synthetic locust ion transport peptide (ITP). Insect Biochem Mol Biol. 1999; 29:11–18. [PubMed: 10070740]

Kratsios P, Stolfi A, Levine M, Hobert O. Coordinated regulation of cholinergic motor neuron traits through a conserved terminal selector gene. Nat Neurosci. 2011; 15:205–214. [PubMed: 22119902]

LaJeunesse DR, Johnson B, Presnell JS, Catignas KK, Zapotoczny G. Peristalsis in the junction region of the *Drosophila* larval midgut is modulated by DH31 expressing enteroendocrine cells. BMC Physiol. 2010; 10:14. [PubMed: 20698983]

Langmead B, Trapnell C, Pop M, Salzberg SL. Ultrafast and memory-efficient alignment of short DNA sequences to the human genome. Genome Biol. 2009; 10:R25. [PubMed: 19261174]

Lee KS, You KH, Choo JK, Han YM, Yu K. *Drosophila* short neuropeptide F regulates food intake and body size. J Biol Chem. 2004; 279:50781–50789. [PubMed: 15385546]

Lee T, Luo L. Mosaic analysis with a repressible cell marker for studies of gene function in neuronal morphogenesis. Neuron. 1999; 22:451–461. [PubMed: 10197526]

Losada-Pérez M, Gabilondo H, del Saz D, Baumgardt M, Molina I, León Y, Monedero I, Díaz-Benjumea F, Torroja L, Benito-Sipos J. Lineage-unrelated neurons generated in different temporal windows and expressing different combinatorial codes can converge in the activation of the same terminal differentiation gene. Mech Dev. 2010; 127:458–471. [PubMed: 20732418]

McQuilton P, St Pierre SE, Thurmond J, FlyBase Consortium. FlyBase 101--the basics of navigating FlyBase. Nucleic Acids Res. 2012; 40:D706–14. [PubMed: 22127867]

Miguel-Aliaga I, Thor S. Segment-specific prevention of pioneer neuron apoptosis by cell-autonomous, postmitotic Hox gene activity. Development. 2004; 131:6093–6105. [PubMed: 15537690]

Mills JC, Taghert PH. Scaling factors: transcription factors regulating subcellular domains. Bioessays. 2012; 34:10–16. [PubMed: 22028036]

Nambu JR, Lewis JL, Wharton KA, Crews ST. The Drosophila *single-minded* gene encodes a helix-loop-helix protein which acts as a master regulator of CNS midline development. Cell. 1991; 67:1157–1167. [PubMed: 1760843]

Nässel DR, Homberg U. Neuropeptides in interneurons of the insect brain. Cell Tissue Res. 2006; 326:1–24. [PubMed: 16761145]

Park D, Veenstra JA, Park JH, Taghert PH. Mapping peptidergic cells in *Drosophila*: where DIMM fits in. PLoS One. 2008; 3:e1896. [PubMed: 18365028]

Sonnenfeld MJ, Jacobs JR. Apoptosis of the midline glia during *Drosophila* embryogenesis: a correlation with axon contact. Development. 1995; 121:569–578. [PubMed: 7768193]

Terhzaz S, O'Connell FC, Pollock VP, Kean L, Davies SA, Veenstra JA, Dow JA. Isolation and characterization of a leucokinin-like peptide of *Drosophila melanogaster*. J Exp Biol. 1999; 202:3667–3676. [PubMed: 10574744]

Trapnell C, Pachter L, Salzberg SL. TopHat: discovering splice junctions with RNA-Seq. Bioinformatics. 2009; 25:1105–1111. [PubMed: 19289445]

Trapnell C, Williams BA, Pertea G, Mortazavi A, Kwan G, van Baren MJ, Salzberg SL, Wold BJ, Pachter L. Transcript assembly and quantification by RNA-Seq reveals unannotated transcripts and isoform switching during cell differentiation. Nat Biotechnol. 2010; 28:511–515. [PubMed: 20436464]

Truman JW, Bate M. Spatial and temporal patterns of neurogenesis in the central nervous system of *Drosophila melanogaster*. Dev Biol. 1988; 125:145–157. [PubMed: 3119399]

Ubink R, Calza L, Hökfelt T. *'Neuro'-peptides in glia*: Focus on NPY and galanin. Trends Neurosci. 2003; 26:604–609. [PubMed: 14585600]

Vasenkova I, Luginbuhl D, Chiba A. Gliopodia extend the range of direct glia-neuron communication during the CNS development in *Drosophila*. Mol Cell Neurosci. 2006; 31:123–130. [PubMed: 16298140]

Veelaert D, Devreese B, Schoofs L, Van Beeumen J, Vanden Broeck J, Tobe SS, De Loof A. Isolation and characterization of eight myoinhibiting peptides from the desert locust, *Schistocerca gregaria*: new members of the cockroach allatostatin family. Mol Cell Endocrinol. 1996; 122:183–190. [PubMed: 8902848]

Wheeler SR, Kearney JB, Guardiola AR, Crews ST. Single-cell mapping of neural and glial gene expression in the developing *Drosophila* CNS midline cells. Dev Biol. 2006; 294:509–524. [PubMed: 16631157]

Wheeler SR, Stagg SB, Crews ST. Multiple *Notch* signaling events control *Drosophila* CNS midline neurogenesis, gliogenesis and neuronal identity. Development. 2008; 135:3071–3079. [PubMed: 18701546]

Wheeler SR, Banerjee S, Blauth K, Rogers SL, Bhat MA, Crews ST. Neurexin IV and Wrapper interactions mediate *Drosophila* midline glial migration and axonal ensheathment. Development. 2009a; 136:1147–1157. [PubMed: 19270173]

Wheeler SR, Stagg SB, Crews ST. MidExDB: a database of *Drosophila* CNS midline cell gene expression. BMC Dev Biol. 2009b; 9:56. [PubMed: 19903351]

Wheeler SR, Pearson JC, Crews ST. Time-lapse imaging reveals stereotypical patterns of *Drosophila* midline glial migration. Dev Biol. 2012; 361:232–244. [PubMed: 22061481]

Xiao H, Hrdlicka LA, Nambu JR. Alternate functions of the *single-minded* and *rhomboid* genes in development of the *Drosophila* ventral neuroectoderm. Mech Dev. 1996; 58:65–74. [PubMed: 8887317]

- *Drosophila* embryonic CNS midline cells were FACS purified followed by RNA-seq

- The midline transcriptome was determined at two major developmental time points

- In situ hybridization revealed diversity of midline neural function gene expression

- 9 neuropeptides and 44 neurotransmitter receptors are present in midline cells

- *castor* regulates neuropeptide gene expression in a midline interneuron subtype
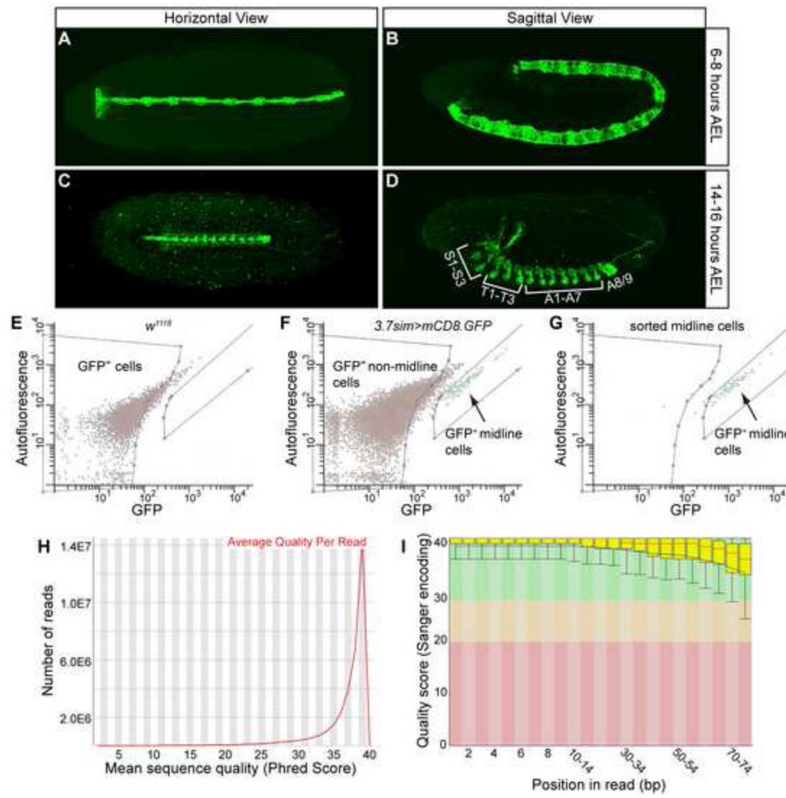
Fig. 1.
High-quality RNA-seq reads were obtained from purified CNS midline cells. (A–D) *3.7sim>mCD8.GFP* embryos were stained with anti-GFP (green) and imaged by confocal microscopy. Images represent (A,C) horizontal views and (B,D) sagittal views of (A,B) 6–8 hour AEL embryos and (C,D) 14–16 hour AEL embryos. (C) The speckled GFP signal seen outside of the midline is from mVUM neurites. (D) Midline expression of GFP is present in all midline cells from segments S1 to A8/9. (E–G) Representative histograms plotting fluorescence profiles of cells from (E) dissociated w^{1118} embryos, (F) dissociated *3.7sim>mCD8.GFP* embryos, and (G) sorted GFP-positive cells from *3.7sim>mCD8.GFP* embryos. Purities of >95% were achieved in sorting GFP-positive cells. Boxes indicate gates used for sorting GFP− and GFP+ cells. (H,I) Representative charts generated using FastQC depicting: (H) the average quality of individual sequencing reads, and (I) the quality of base calls at each position in a sequencing read across all reads.
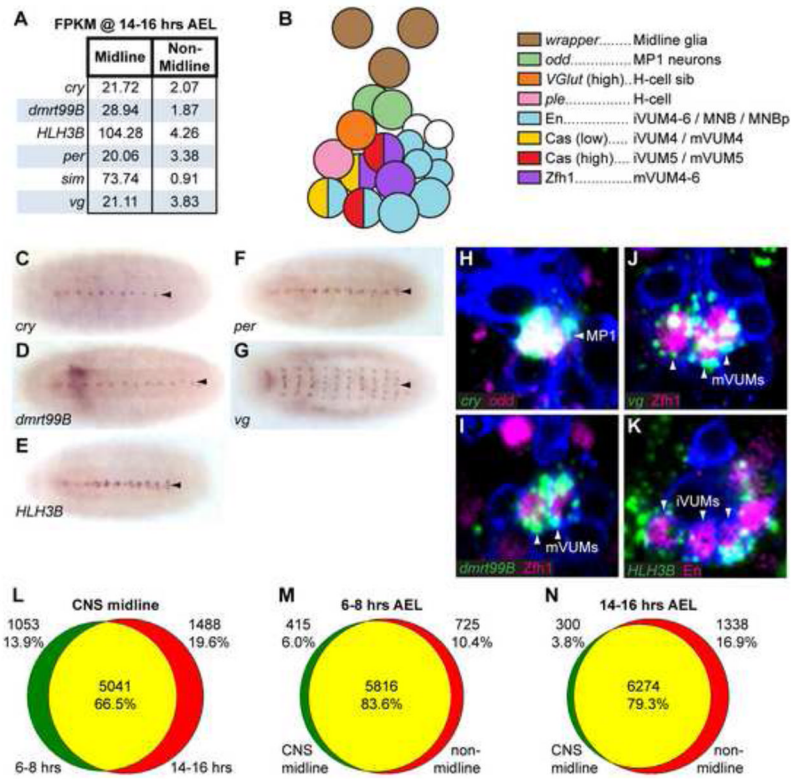
Fig. 2.
RNA-seq data accurately predicts CNS midline-enriched gene expression. (A) List showing 14–16 hour midline and non-midline FPKM values for 6 genes with enriched midline expression. (B) Diagram of a typical stage 16/17 midline segment showing midline cells depicted with the cell-type specific markers used in this manuscript. Anterior left, dorsal top. (C–G) Alkaline phosphatase in situ hybridization experiments of stage 16 whole-mount embryos showing strong CNS midline enrichment of (C) *cry*, (D) *dmrt99B*, (E) *HLH3B*, (F) *per*, and (G) *vg*. Horizontal views are shown, with anterior left. (H–K) Stage 16/17 *3.7sim>mCD8.GFP* embryos were stained with anti-GFP to visualize midline cells (blue), and hybridized with RNA probes (lower-case italics) or immunostained with antibodies (upper-case, non-italicized). Each image is a 1 μm confocal slice showing a sagittal view of the relevant portion of a single segment with anterior left and dorsal top. (H) *cry* colocalizes with *odd* in MP1 neurons. (I) *dmrt99B* and (J) *vg* colocalize with Zfh1 in mVUMs. Only 2 mVUMs can be seen in the confocal plane shown in (I). (K) *HLH3B* colocalizes with En in iVUMs. Non-midline *HLH3B* expression is also seen in this image. (L–N) Venn diagrams illustrating the extent of overlap of genes expressed with FPKM values 5 between: (L) the 6–8 hour (green) and 14–16 hour (red) midline samples; (M) midline (green) and non-midline (red) cells at 6–8 hours AEL; and (N) midline (green) and non-midline (red) cells at 14–16 hours AEL.
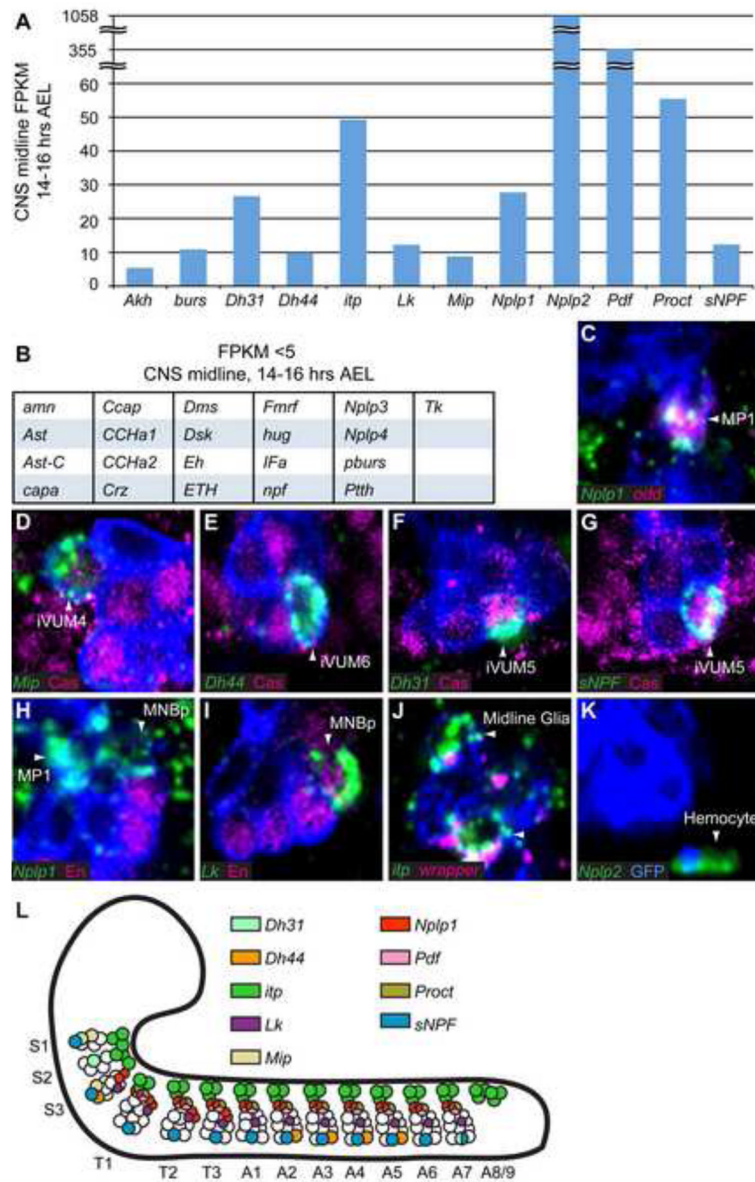
Fig. 3.
Neuropeptide precursor gene expression in the CNS midline cells. (A) 12 neuropeptide precursor genes have CNS midline FPKM values 5 at 14–16 hours AEL, while (B) 21 genes have FPKM values <5. (C–K) In situ hybridization of 8 neuropeptide precursor genes (green) are shown in sagittal views of stage 16/17 *3.7sim>GFP* embryos. (C,H–K) mCD8.GFP was detected with anti-GFP (blue), and (D–G) tau.GFP was detected with anti-Tau (blue). Various midline cell markers are shown in magenta, and arrowheads indicate the neuropeptide gene-expressing cells. Anterior left, dorsal top. (C) *Nplp1* is expressed in *odd*^{+} MP1 neurons. (D) *Mip* is expressed in Cas[lo] iVUM4, (E) *Dh44* in Cas[−] iVUM6, and (F) *Dh31* and (G) *sNPF* in Cas^{hi} iVUM5 neurons. (H) *Nplp1* is also expressed in an En[−] MNBp neuron, while (I) *Lk* is expressed in an En[+] MNBp neuron. (J) Expression of *itp* is in *wrapper*[+] AMG. (K) *Nplp2* expression is seen in hemocytes that have engulfed apoptotic *GFP*-expressing midline cells. (L) Diagram of segmental neuropeptide expression in the CNS midline at 14–16 hours AEL.
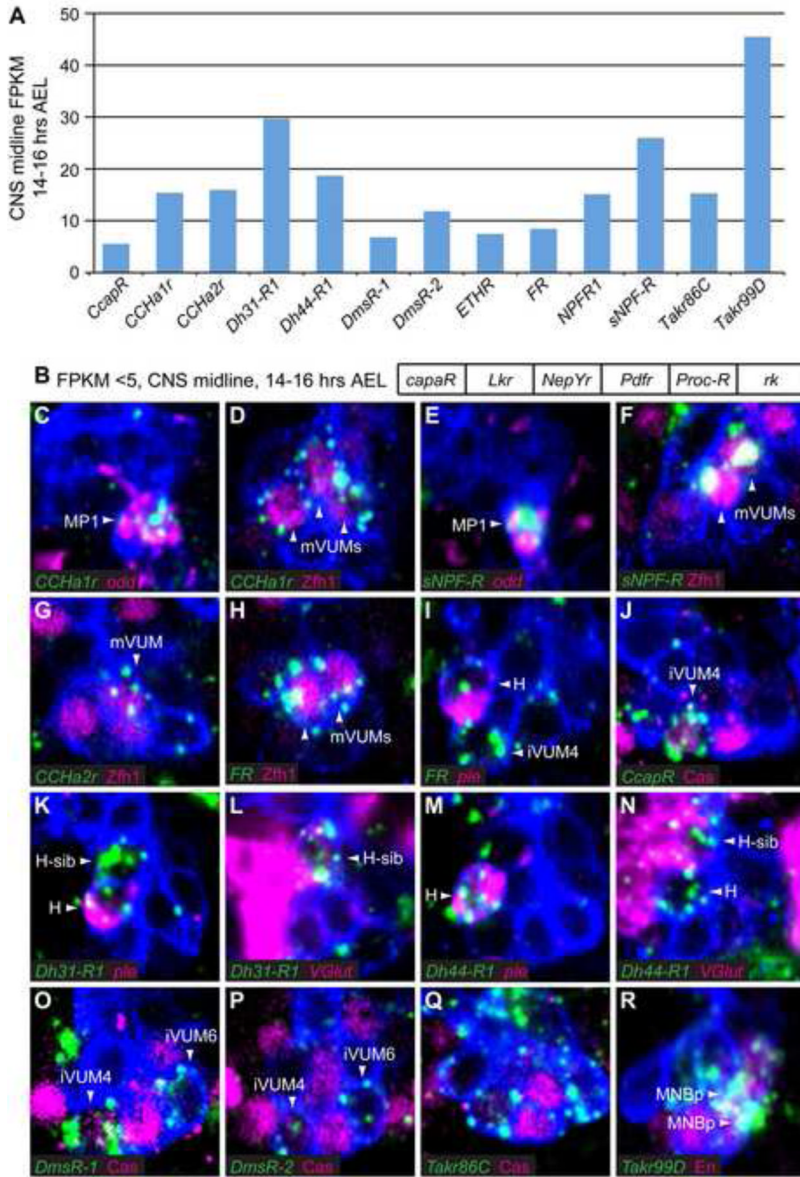
Fig. 4.
Neuropeptide receptor expression in the CNS midline cells. (A) 13 neuropeptide receptor genes have CNS midline FPKM values 5 at 14–16 hours, while (B) 6 neuropeptide receptor genes have FPKM values <5. (C–R) In situ hybridization of 11 neuropeptide precursor genes (green) are shown in sagittal views of stage 16/17 *3.7sim>GFP* embryos. (C–I,K–N,R) mCD8.GFP was detected with anti-GFP (blue), and (J,O–Q) tau.GFP was detected with anti-Tau (blue). Midline cell markers are shown in magenta. Arrowheads indicate the neuropeptide receptor-expressing cells. Anterior left, dorsal top. (C,E) *CCHa1r* and *sNPF-R* expression is present in MP1 neurons. (D,F–H). *CCHa1r*, *sNPF-R*, *CCHa2r*, and *FR* expression is present in mVUMs. (I) *FR* expression is also present in H-cell and iVUM4 of several segments. (J) *CcapR* is expressed in Cas^lo iVUM4. (K,M) *Dh31-R1* and *Dh44-R1* colocalize with *ple* in H-cell neurons and (L,N) with high *VGlut* in H-cell sib neurons. (O,P) Expression of *DmsR-1* and *DmsR-2* is observed in Cas^lo iVUM4 and Cas⁻

iVUM6. (Q,R) *Takr86C* and *Takr99D* expression is present in most midline neurons with *Takr99D* expression highest in the MNBp (arrowheads).
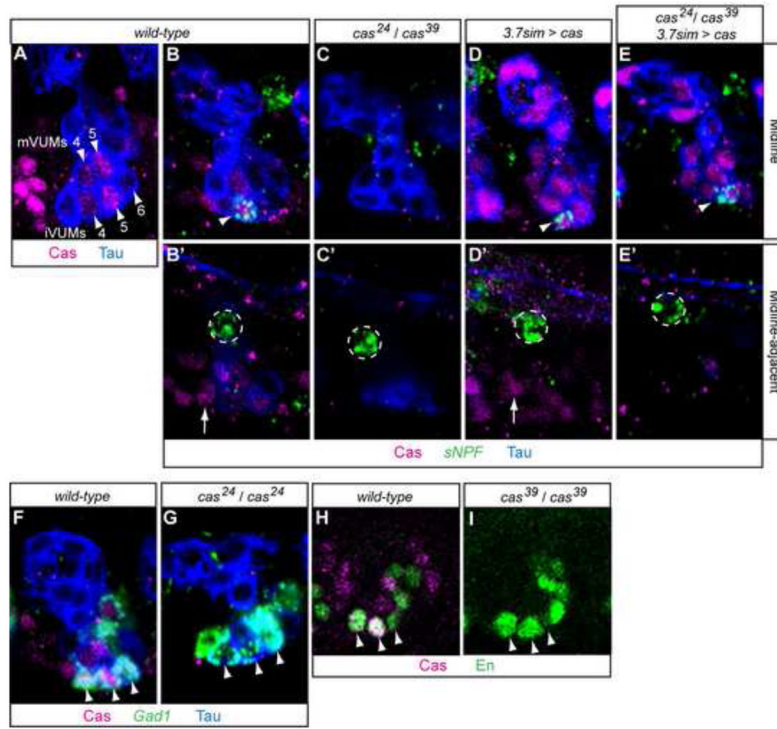
Fig. 5.
Expression of *sNPF* in iVUM5 is regulated by *cas*. Sagittal views of stage 16/17 *3.7sim-Gal4 UAS-tau.GFP* embryos showing a sagittal view of a single segment of the (A–G) CNS midline cells or (B′-E′) corresponding slices ~8 µm lateral to the midline. Embryos are stained with anti-Tau (blue) and anti-Cas (magenta) and hybridized to (B–E) an *sNPF* probe (green) or (F,G) a *Gad1* probe. In wild-type embryos, *sNPF* expression is (B) present in iVUM5 (arrowhead), and (B′) present in a lateral CNS Cas⁻ cell (dotted circle). Arrow shows non-midline Cas protein in wild-type embryos. (C) In *cas²⁴/cas³⁹* mutant embryos, *sNPF* expression is absent in iVUM5, although (C′) *sNPF* is present in lateral neurons (dotted circle). (D,D′) In *3.7sim-Gal4 UAS-tau.GFP/UAS-cas*, misexpression of *cas* occurs in all midline cells, yet has no effect on *sNPF* expression. (E,E′) In *3.7sim-Gal4 UAS-tau.GFP/UAS-cas; cas²⁴/cas³⁹*, misexpression of *cas* throughout the CNS midline in a *cas* mutant background rescues CNS midline expression of *sNPF* in iVUM5 (arrowhead). (F) In a wild-type embryo, *Gad1* is expressed at high levels in iVUM4-6 (arrowheads) and MNBp. (G) In *cas²⁴* mutant embryos, *Gad1* expression is unaffected and is present in all iVUMs, including iVUM5. (H,I) In both (H) wild-type and (I) *cas³⁹* mutant embryos, En is present in iVUM neurons (arrowheads). Note the absence of Cas immunostaining in panels G and I indicating that these embryos were homozygous mutant for *cas*.

Table 1

Summary of FACS and RNA-seq. For each sample, the numbers of cells isolated via FACS, 76 nucleotide sequencing reads generated from the cDNA library, and reads mapping uniquely to the genome are shown.

Sample Name	Cell Population	Time-point	# of Sorted Events (Cells)	# of Reads Generated	# of Uniquely Mapped Reads
6Mid1	CNS Midline	6–8 hours AEL	20,000	7,162,776	4,471,612
6Mid2	CNS Midline	6–8 hours AEL	40,000	8,179,000	6,213,434
6Mid1+2	CNS Midline	6–8 hours AEL	N/A	N/A	10,701,922
6nonMid	Non-Midline	6–8 hours AEL	50,000	8,923,570	6,062,148
14Mid1	CNS Midline	14–16 hours AEL	42,000	23,995,806	10,363,609
14Mid2	CNS Midline	14–16 hours AEL	62,000	29,547,037	23,829,053
14Mid1+2	CNS Midline	14–16 hours AEL	N/A	N/A	34,209,443
14nonMid	Non-Midline	14–16 hours AEL	50,000	23,758,803	15,216,077

Table 2

Midline FPKM values for small-molecule neurotransmitter receptors at 14–16 hours AEL. Genes with FPKM values ≥5 are shown on left, and those with FPKM values <5 are shown on right.

14–16 hr midline FPKM ≥5						14–16 hr midline FPKM <5	
Symbol	FPKM	Gene Symbol	FPKM	Gene Symbol	FPKM	Gene Symbol	FPKM
5-HT1A	74.82	GABA-B-R3	10.03	nAcRα-96Ab	100.85	clumsy	1.12
5-HT1B	8.52	gfA	36.58	nAcRβ-21C	7.41	GluRIIA	1.08
5-HT2	5.44	Glu-RI	50.34	nAcRβ-64B	264.02	GluRIIB	0.13
5-HT7	15.43	Lcch3	83.81	nAcRβ-96A	97.23	GluRIIC	0.89
CG3822	88.53	mAcR-60C	73.04	Nmdar1	69.71	HisCl1	1.01
CG42796	5.21	mGluRA	7.67	Nmdar2	77.55	ort	0.16
D2R	50.92	nAcRα-30D	87.68	Oamb	20.64	TyrR	2.54
DopR	10.49	nAcRα-34E	109.21	Octβ2R	62.22		
DopR2	6.58	nAcRα-7E	10.03	Rdl	166.58		
GABA-B-R1	39.71	nAcRα-80B	9.04				
GABA-B-R2	87.69	nAcRα-96Aa	174.64				